A simplified design approach to prevent shrinkage cracking in patch repairs

O'FLAHERTY, Fin and MANGAT, P. S.

Published version

O'FLAHERTY, Fin and MANGAT, P. S. (2006). A simplified design approach to prevent shrinkage cracking in patch repairs. Magazine of concrete research, 58 (1), 31-42.

Magazine of Concrete Research, 2006, **58**, No. 1, February, 31–42

A simplified design approach to prevent shrinkage cracking in patch repairs

F. J. O'Flaherty* and P. S. Mangat*

Sheffield Hallam University

This paper outlines two procedures for determining the interfacial shrinkage stresses in a repair patch. The first is an analytical approach based on the analogy of a bimetallic strip undergoing contraction (shrinkage). The second is a semi-empirical procedure based on strain monitoring of in situ repairs to in-service bridges. The procedures determine conversion factors to relate the specified properties of the repair materials to their in situ properties in a field repair patch. For example, the shrinkage of a repair patch is influenced by the volume–surface effect, site temperature and relative humidity which are not considered in repair material specification. Creep is initiated in situ by differential shrinkage stresses in the repair material and is determined by adopting an effective elastic modulus approach. Both procedures require the basic material properties (elastic modulus, shrinkage, creep) and geometrical details (width, depth) of the repair patch. The analytical approach incorporates the repair material creep coefficient to predict the interfacial tensile stresses. Alternatively, it uses a less rigorous, elastic approach that omits creep. The creep approach provides higher accuracy whereas the elastic approach overestimates stresses since relaxation by creep is neglected. The elastic approach is recommended for design due to its simplicity and the in-built factor of safety provided by the overestimation of tensile stress. The semi-empirical approach uses an expression derived from long-term field data to determine the strain (and consequently stresses) at the interface of the repair patch and the substrate concrete. The procedures predict the maximum interfacial tensile stress during the service life of a repair patch. They can be used to design crack-free repair patches and optimise repair material selection through a better understanding of the interaction between the repair patch and substrate concrete.

Notation

b	breadth of the in situ repair material or substrate concrete
d_{rm}	depth of the in situ repair material
d_{sub}	depth, or zone of influence of the substrate concrete affected by shrinkage strain transfer
E	elastic modulus ($= \sigma/\varepsilon$)
E_{rm}	28-day compressive elastic modulus of the repair material
$E_{rm(t)}$	elastic modulus of the repair material at age t
$E_{rm(eff)}$	effective elastic modulus of the repair material
$E_{rm(eff),t}$	effective elastic modulus of the repair material at age t
E_{sub}	compressive elastic modulus of the substrate concrete
F_{shr}	restrained shrinkage force in the in situ repair patch
$f_{cu(t)}$	average compressive strength of a repair material at any age t
$f_{cu(7)}$	average compressive strength of a repair material at 7 days
$f_{cu(14)}$	average compressive strength of a repair material at 14 days
$f_{cu(28)}$	average compressive strength of a repair material at 28 days
$f_{cu(90)}$	average compressive strength of a repair material at 90 days
$f_{cu(182)}$	average compressive strength of a repair material at 182 days
G1	repair material G1
I_{rm}	second moment of area of the in situ repair material ($= bd_{rm}^3/12$)
I_{sub}	second moment of area of the substrate concrete ($= bd_{sub}^3/12$)
k	constant for temperature correction

* Centre for Infrastructure Management, Sheffield Hallam University, City Campus, Pond Street, Sheffield S1 1WB,UK.

(MCR 41335) Paper received 22 December 2004; last revised 20 June 2005; accepted 6 September 2005.

L2	repair material L2
L3	repair material L3
L4	repair material L4
$M_{rm(shr)}$	moment in the repair material due to restrained shrinkage strain effects
$M_{sub(shr)}$	moment in the substrate concrete due to restrained shrinkage strain transfer
m	modular ratio ($= E_{rm}/E_{sub}$)
R	radius of curvature of the repair patch
RH	relative humidity in situ
$RS_{(field)}$	relative shrinkage of the repair material in the in situ repair patch
$RS_{(lab)}$	relative shrinkage of the repair material in the laboratory
subs	substrate concrete
$T_{(field)}$	temperature of the field repair patch in °C
t	time in days
v/s	volume/surface ratio
α	constant for relative humidity correction
β_1	conversion factor for volume/surface correction
β_2	conversion factor for temperature correction
β_3	conversion factor for relative humidity correction
$\beta_{4(t)}$	elastic modulus conversion factor for age
$\beta_{5(t)}$	elastic modulus conversion factor for early age creep
ε	strain ($= \sigma/E$)
$\varepsilon_{rm(bend)}$	strain in the repair material due to moment $M_{rm(shr)}$
$\varepsilon_{rm(dir)}$	strain in the repair material due to restrained shrinkage force, F_{shr}
$\varepsilon_{rm(shr)}$	restrained shrinkage strain in the repair material
$\varepsilon_{rm(tens)}$	virtual tensile strain in the repair material due to partial restraint to shrinkage
$\varepsilon_{shr(field)}$	free shrinkage of the in situ repair patch in the field
$\varepsilon_{shr(lab)}$	free shrinkage of the repair material in the laboratory
$\varepsilon_{sub(dir)}$	strain in the substrate concrete due to restrained shrinkage force, F_{shr}
$\varepsilon_{sub(shr)}$	shrinkage strain transferred to the substrate concrete
η	constant for relative humidity correction
λ	percentage of shrinkage strain transferred to the substrate concrete
σ	stress $= (\varepsilon E)$
$\sigma_{rm(bend)}$	tensile stress at the interface of the repair material due to moment $M_{rm(shr)}$
$\sigma_{rm(shr)}$	interfacial tensile stress in the repair material due to restrained shrinkage strain
$\sigma_{sub(bend)}$	compressive stress at the interface of the substrate concrete due to moment $M_{sub(shr)}$
$\sigma_{sub(shr)}$	interfacial compressive stress in the substrate concrete due to shrinkage strain transfer
φ	creep coefficient of the repair material
$\varphi_{(t)}$	creep coefficient of the repair material at age t
$\sigma_{t(t)}$	estimated tensile strength of the in situ repair materials
°C	temperature in degrees Celsius

Introduction

In recent times, the issue of durability of concrete repairs has replaced strength as the main criterion for the design of patch repairs,[1] since a repair material must not only restore the structural integrity of the member, but also must serve as a durable barrier against the ingress of chlorides and carbon dioxide to arrest further steel reinforcement corrosion. However, before a repair system can be specified, the interaction between the repair material and the concrete substrate must be understood to ensure that the repair system will function properly without cracking. It is well established that repair materials are prone to volume change due to shrinkage and creep; control of these properties is crucial to prevent cracking caused by tensile stresses induced by restrained shrinkage.[2,3] Recent research shows that the most important properties for efficient structural interaction are elastic modulus, shrinkage and creep,[4,5] A repair material with a fully developed elastic modulus greater than that of the substrate concrete (i.e. $E_{rm} > E_{sub}$ at 28 days) will perform satisfactorily in the long term. The stiffer repair material transfers shrinkage strain to the less stiff substrate concrete with optimum transfer being achieved at $E_{rm} \sim 1{\cdot}3E_{sub}$.

A repair material is most susceptible to cracking in the first few weeks after application if it possesses high shrinkage characteristics (shrinkage is considered to be high if greater than 0·1%).[6] During this early period, the elastic modulus of the repair material is developing and shrinkage transfer to the substrate concrete does not take place since $E_{rm} < E_{sub}$. Simultaneously, cementitious materials exhibit higher creep at early ages. The resulting tensile creep of the repair material in a patch repair will relax the tensile stress due to the restraint to shrinkage provided by the substrate concrete.

Procedures for interfacial shrinkage stress analysis

Introduction

The purpose of this paper is to assist repair technologists in the design of patch repairs. The design procedures developed in the paper are validated against full-scale field trials of repair patches with known material properties and geometric details. The creep approach incorporates the creep coefficient of the repair material in the prediction of the interfacial stresses. This is the most accurate method and is recommended where a precise estimation of stresses is required. A less rigorous approach is the elastic method where the creep

characteristics of the repair material are excluded from the analysis. This approach is important in current practice because the creep data of the repair materials are not normally available from the suppliers. The elastic approach predicts higher interfacial tensile stress because relaxation through creep is neglected. However, the overestimation of stresses owing to the omission of creep provides an in-built factor of safety in the design of patch repairs. The elastic approach is, therefore, recommended for the design of patch repairs owing to its simplicity and easy application in practice.

Analytical procedure

The mechanics of patch repair interaction with the substrate concrete, based on an analogy of the bimetallic strip undergoing a drop in temperature, were developed elsewhere by the authors.[7] Simultaneous equations were derived to estimate both the interfacial tensile stress in the repair material and the compressive stress in the substrate concrete for any repair patch. The analysis requires the properties of the repair material (elastic modulus, shrinkage and tensile creep), substrate concrete (elastic modulus) and geometrical details of the repair patch (width, depth of repair material and substrate concrete). Details are presented elsewhere[7] but the key information is summarised here.

Figure 1 shows a cross-section through an unpropped compression member, repaired with a material with $E_{rm} > E_{sub}$ (the influence of steel reinforcement is omitted for simplicity and to aid clarity). Immediately after application and before shrinkage begins, the repair material extends the full length of the repair patch, labelled level 0 to level 1. Assuming the substrate concrete has a negligible elastic modulus ($E_{rm} \approx 0$), the repair material would shrink freely over a period of time from level 0 to level 2 in Fig. 1, displaying a free shrinkage strain, $\varepsilon_{shr(field)}$. In an actual repair situation, the substrate concrete has a stiffness which, in the case being considered, is less than the stiffness of the repair material ($E_{sub} < E_{rm}$). The repair material, therefore, is prevented from deforming freely owing to the partial restraint provided by the substrate concrete. The maximum restraint will be at the substrate/repair material interface, but will gradually reduce as the distance from the interface increases owing to the action of the normal compressive stresses acting within the zone of influence (these stresses were not considered since the focus of the paper is the interfacial zone between the repair material and substrate concrete where the tensile cracking of the repair material is of critical concern in the design of patch repairs). Bending in the form of a circular arc will occur owing to the restrained shrinkage forces, F_{shr}, at the interface as shown in Fig. 1. A tensile force is mobilised in the repair material and a compressive force acts in the substrate concrete.

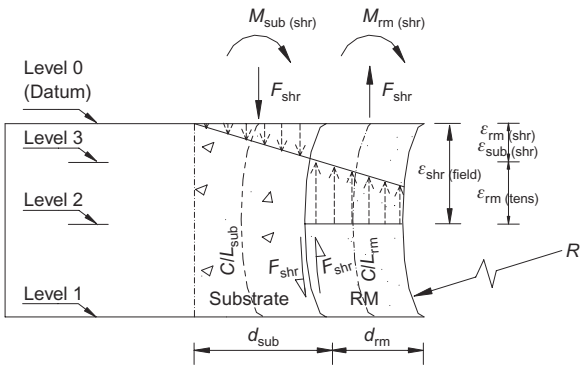

Fig. 1. Idealised forces due to distribution of shrinkage strain

The repair material is, therefore, assumed to shrink from level 0 to level 3 at the interface, $\varepsilon_{rm(shr)}$, Fig. 1. The interfacial bond (assuming no slip) enables the substrate concrete to deform also from level 0 to level 3, $\varepsilon_{sub(shr)}$. A tensile strain $\varepsilon_{rm(tens)}$ will, therefore, result in the repair material and is equal to the difference between $\varepsilon_{shr(field)}$ and $\varepsilon_{rm(shr)}$. A strain gradient will be evident across the repair patch and the zone of influence in the substrate concrete. The internal force system for both the repair material and substrate concrete can be reduced to longitudinal forces acting along each centroidal axis, F_{shr} (tension and compression respectively) plus bending moments ($M_{rm(shr)}$ and $M_{sub(shr)}$), Fig. 1. These bending moments will be produced by the eccentric interfacial forces, F_{shr} acting at $d_{sub}/2$ and $d_{rm}/2$ respectively from the centroidal axis of the substrate concrete and the repair, that is $M_{rm(shr)} = (F_{shr})(d_{rm}/2)$ and $M_{sub(shr)} = F_{shr})(d_{sub}/2)$.

The depth of concrete substrate (d_{sub}) influenced by shrinkage strain transfer is calculated from the radius of curvature of the deflection, R, which is caused by shrinkage restraint provided by the substrate to the repair patch.[7] Since R is large compared with the cross-section dimensions of the zone of influence and repair patch, it can therefore be taken as the same for both from elastic theory of bending

$$\frac{1}{R_{rm}} = \frac{1}{R_{sub}} \tag{1}$$

Equation (1) can be re-written in the form

$$\frac{M_{sub(shr)}}{E_{sub} I_{sub}} = \frac{M_{rm(shr)}}{E_{rm} I_{rm}} \tag{2}$$

Substituting for $M_{rm(shr)} = (F_{shr})(d_{rm}/2)$, $M_{sub(shr)} = (F_{shr})(d_{sub}/2)$, $I_{sub} = [b(1/12)d_{sub}^3]$ and $I_{rm} = [b(1/12)d_{rm}^3]$ and expanding the second moment of area terms in equation (2) gives

$$\frac{F_{shr}(d_{sub}/2)}{E_{sub}[b(1/12)d_{sub}^3]} = \frac{F_{shr}(d_{rm}/2)}{E_{rm}[b(1/12)]d_{rm}^3} \tag{3}$$

Simplifying equation (3) gives

$$d_{sub}^2 = d_{rm}^2 \frac{E_{rm}}{E_{sub}} \tag{4}$$

Replacing E_{rm}/E_{sub} with m in equation (4) and simplifying, the depth of substrate concrete, d_{sub}, affected by the transfer of shrinkage strain can be obtained from

$$d_{sub} = d_{rm}\sqrt{m} \tag{5}$$

Referring to Fig. 1, the perpendicular distance between the forces F_{shr} is $\frac{1}{2}(d_{rm} + d_{sub})$. The couple produced by these forces must, for equilibrium, balance the sum of the moments in the repair and substrate materials. Thus

$$\frac{F_{shr}}{2}(d_{sub} + d_{rm}) = M_{sub(shr)} = M_{rm(shr)} \tag{6}$$

From the elastic theory of bending, $M_{sub(shr)} = (E_{sub}I_{sub})/R$ and $M_{rm(shr)} = (E_{rm}I_{rm}/R)$, where R = radius of curvature and I_{sub} and I_{rm} are as given in equation (3) (Fig. 1). Therefore, equation (6) can be written as

$$\frac{F_{shr}}{2}(d_{sub} + d_{rm}) = \frac{E_{sub}I_{sub}}{R} + \frac{E_{rm}I_{rm}}{R} \tag{7}$$

Rearranging equation (7) gives

$$F_{shr} = 2\left(\frac{E_{sub}I_{sub} + E_{rm}I_{rm}}{d_{sub} + d_{rm}}\right)\frac{1}{R} \tag{8}$$

The only unknowns in equation (8) are the force due to shrinkage, F_{shr}, and the radius of curvature caused by bending, R.

A second relationship was obtained by considering the strain compatibility of the two materials (repair and substrate) at the interface. These strains are made up of three components

(*a*) the elastic strain due to the longitudinal forces, F_{shr}
(*b*) the elastic strains due to the moments $M_{sub(shr)}$ and $M_{rm(shr)}$
(*c*) the free shrinkage of the repair material in the field $\varepsilon_{shr(field)}$.

Creep strains in the repair material are neglected at this stage but are considered later.

With regard to the elastic strains due to the direct shrinkage force, F_{shr}, the strains in the substrate concrete and repair material are obtained from $\varepsilon = \sigma/E$, therefore

$$\varepsilon_{sub(dir)} = \frac{F_{shr}}{bd_{sub}E_{sub}} \tag{9}$$

and

$$E_{rm(dir)} = \frac{F_{shr}}{bd_{rm}E_{rm}} \tag{10}$$

The elastic strains at the substrate/repair interface due to the moments $M_{sub(shr)}$ and $M_{rm(shr)}$ are determined from the elastic theory of bending. It can be shown that

$$\sigma_{sub(bend)} = \frac{d_{sub}E_{sub}}{2R} \tag{11}$$

and

$$\sigma_{rm(bend)} = \frac{d_{rm}E_{rm}}{2R} \tag{12}$$

Dividing equations (11) and (12) by the elastic modulus of the respective material gives the strain in each material, $\varepsilon_{sub(bend)} = d_{sub}/2R$ and $\varepsilon_{rm(bend)} = d_{rm}/2R$ respectively.

At the common interface between the repair material and substrate concrete, the net strain in the substrate concrete is equal to net strain in the repair material. Therefore

$$\left[\frac{F_{shr}}{bd_{sub}E_{sub}}\right] = \frac{d_{sub}}{2R}$$

$$= \varepsilon_{shr(field)} - \left[\frac{F_{shr}}{bd_{rm}E_{rm}}\right] - \frac{d_{rm}}{2R} \tag{13}$$

Equation (13) can be rearranged to give

$$F_{shr} = \frac{\{\varepsilon_{shr(field)} - [(1/2R)(d_{sub} + d_{rm})]\}b}{\left(\frac{1}{d_{sub}E_{sub}} + \frac{1}{d_{rm} + E_{rm}}\right)} \tag{14}$$

Equations (8) and (14) can be solved to determine the only unknowns F_{shr} and R. Hence, the compressive stress at the interface of the substrate concrete due to a transfer of shrinkage strain from the stiffer repair material can be determined as

$$\sigma_{sub(shr)} = \frac{F_{shr}}{b\sqrt{m}d_{rm}} = \frac{E_{sub}\sqrt{m}d_{rm}}{2R} \tag{15}$$

Similarly, the tensile stress in the repair material (at the interface) can be obtained from

$$\sigma_{rm(shr)} = -\frac{F_{shr}}{b_{drm}} - \frac{E_{rm}d_{rm}}{2R} \tag{16}$$

For simplicity, the above approach does not take creep into account. This provides a significant overestimation of tensile stress by a factor of about two (see section on 'validation', below) compared with analysis including creep data.[7] However, a more accurate estimation of stress can be made by replacing E_{rm} (equation (16)) with an effective elastic modulus, $E_{rm(eff)}$ based on creep data, which accounts for stress relaxation due to creep. Details of the procedure are given in the section on creep, below.

Semi-empirical procedure

Substrate concrete. The semi-empirical procedure estimates interfacial stresses using an empirical relationship between the modular ratio (m) of the repair material and substrate concrete and the percentage of shrinkage strain (λ) transferred to the substrate concrete. $m = E_{rm}/E_{sub}$ where E_{rm} is the 28-day compressive elastic modulus of the repair material and E_{sub} is the compressive elastic modulus of the substrate concrete at the age of repair application, determined in accordance with BS 1881.[8] The empirical relationship

for shrinkage strain transfer to the substrate concrete was obtained from field investigations on in situ repairs to highway structures whose details are given elsewhere.[5] The resulting linear relationship given in Fig. 2 shows that a higher m leads to greater transfer of shrinkage strain from the repair to substrate concrete (at the interface). Optimum transfer is achieved at $m \sim 1{\cdot}32$. The percentage of shrinkage strain transfer (λ) for any repair material with $1{\cdot}0 \leqslant m \leqslant 1{\cdot}32$ can be obtained from the transposed equation of the straight line in Fig. 2

$$\lambda = \frac{m-1}{0{\cdot}0032}(\%) \tag{17}$$

The strain transferred to the substrate concrete, $\varepsilon_{\text{sub(shr)}}$, can be obtained by substituting $\lambda = [\varepsilon_{\text{sub(shr)}}/\varepsilon_{\text{shr(field)}}]$ (100) into equation (17) to give

$$\varepsilon_{\text{sub(shr)}} = \left[\frac{m-1}{0{\cdot}32}\right]\varepsilon_{\text{shr(field)}} \tag{18}$$

where $\varepsilon_{\text{shr(field)}}$ is the free shrinkage of the in situ repair patch in the field.

The section of this paper dealing with properties of repair material outlines the procedure to convert laboratory data on free shrinkage of the repair materials, $\varepsilon_{\text{shr(lab)}}$, to corresponding field data on free shrinkage $\varepsilon_{\text{shr(field)}}$, by accounting for differences in temperature, relative humidity and volume/surface. The interfacial compressive stress in the substrate concrete is given by

$$\sigma_{\text{subs(shr)}} = [\varepsilon_{\text{sub(shr)}}](E_{\text{sub}}) \tag{19}$$

This compressive stress induced by the restrained shrinkage of the repair material is assumed to cause no creep (and hence no creep relaxation) of the substrate concrete since

(*a*) in a repair situation, the concrete substrates have typically been under service load over long periods (e.g. over 30 years) and creep has practically ceased
(*b*) the compressive stresses induced in the substrate concrete due to restrained shrinkage of the repair patch are small (typically < 4 N/mm^2) yielding very low stress/strength ratios of creep loading.

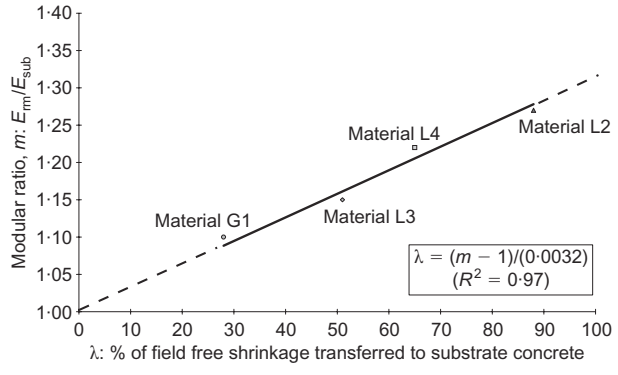

Fig. 2. Relationship between modular ratio, m, and field free shrinkage transferred to the substrate concrete in patch repairs[5]

Repair material. The tensile strain in the repair material, $\varepsilon_{\text{rm(tens)}}$, is the difference between its field free shrinkage, $\varepsilon_{\text{shr(field)}}$, and the shrinkage strain transferred to the substrate concrete $\varepsilon_{\text{sub(shr)}}$, given by equation (18). $\varepsilon_{\text{rm(tens)}}$ can be estimated by modifying equation (18) to give

$$\varepsilon_{\text{rm(tens)}} = \left[\frac{1-(m-1)}{0{\cdot}32}\right]\varepsilon_{\text{shr(field)}} \tag{20}$$

The interfacial tensile stress due to the restraint to shrinkage in the repair material is therefore

$$\sigma_{\text{rm(shr)}} = [\varepsilon_{\text{rm(tens)}}](E_{\text{rm}}) \tag{21}$$

Properties of repair material—conversion of laboratory/material suppliers' data to field data

Introduction

The free shrinkage of a repair material determined in the laboratory under controlled conditions, $\varepsilon_{\text{shr(lab)}}$, will differ from the in situ free shrinkage of the repair material in the field, $\varepsilon_{\text{shr(field)}}$. To enable the prediction of interfacial stress from the procedures presented in this paper, the laboratory data are related to site conditions through the use of conversion factors (β) that take into account the difference in volume/surface ratios, temperature and relative humidity between the in situ and laboratory conditions.

As an illustration, an example is provided to convert the laboratory free shrinkage, creep and elastic modulus data to their equivalent in situ values in a real repair patch. The example is based on an in situ repair patch in a bridge structure investigated previously[7] where a repair material, labelled L4, was used. Basic properties of the material L4 were determined by standard laboratory testing and curing at 20°C, 55%RH. The dimensions of the test specimens were 500 × 100 × 100 mm. The 28-day elastic modulus and the 100-day free shrinkage values were 29·1 kN/mm^2 and 782 microstrain respectively.[8]

Free shrinkage

Volume/surface ratio. A higher volume/surface (v/s) ratio will lead to lower shrinkage and vice versa.[9–11] This was accounted for by applying the nonlinear relationship between relative shrinkage and v/s ratios for concrete as shown in Fig. 3.[12] External exposed surfaces only are used to calculate the surface area of the repair patches, the surface bonded to the substrate concrete is neglected. The v/s ratio is calculated for both the laboratory test specimen and the field repair patch, thus the relative shrinkage

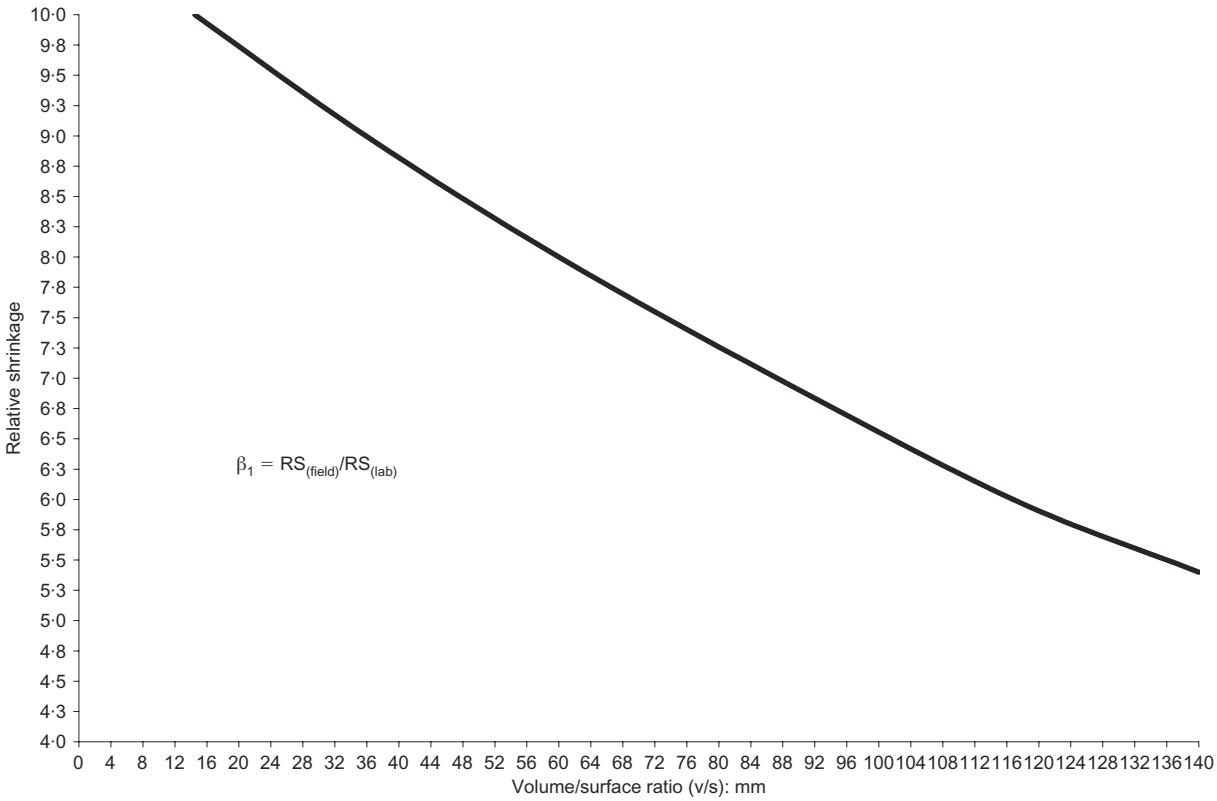

Fig. 3. Shrinkage conversion factor β_1 for different volume/surface ratios

(RS) of the two can be estimated from Fig. 3. The v/s conversion factor (denoted β_1) is given by

$$\beta_1 = \frac{RS_{(field)}}{RS_{(lab)}} \tag{22}$$

The field repair patch of repair material L4 measured $1500 \times 1500 \times 130$ mm, whereas the laboratory specimen used for free shrinkage measurements had the dimensions $500 \times 100 \times 100$ mm. The volumes, therefore, of the field patch repair and laboratory specimen are $292{\cdot}5 \times 10^6$ mm^3 and 5×10^6 mm^3 respectively, whereas the corresponding exposed surface areas are $2{\cdot}25 \times 10^6$ mm^2 and $0{\cdot}22 \times 10^6$ mm^2. The resulting v/s ratios are 130 for the field patch repair and 22·7 for the laboratory specimen. Therefore, using the relationship in Fig. 3 gives the values of $RS_{(field)} \sim 5{\cdot}75$ mm and $RS_{(lab)} \sim 9{\cdot}60$ mm. Hence, from equation (22), $\beta_1 = 5{\cdot}75/9{\cdot}60 = 0{\cdot}6$.

Temperature. Shrinkage was adjusted on the basis that a 1°C fall in site temperature relative to the control laboratory temperature results in a 1% decrease in the free laboratory shrinkage[12] as shown in Fig. 4. The factor for temperature correction is denoted β_2. The best-fit linear equation representing the relationship in Fig. 4 is

$$\beta_2 = 0{\cdot}01(T_{(field)}) + k \tag{23}$$

where $T_{(field)}$ is the temperature of the field repair patch (°C) and k is a constant depending on the temperature at which standard (laboratory) shrinkage testing is conducted. Values of k representing different test temperatures are listed in Fig. 4 and the case for 20°C test temperature ($k = 0{\cdot}8$) is plotted in the graph.

Referring to the practical example of the repair patch made with material L4 considered in this paper, the average field temperature of exposure was 10°C, whereas the laboratory temperature was 20°C. Therefore, from the graph in Fig. 4, the shrinkage modification factor, $\beta_2 \sim 0{\cdot}9$. Alternatively, using equation (23), β_2 can be calculated as $k = 0{\cdot}8$; therefore, $\beta_2 = 0{\cdot}01(10) + 0{\cdot}8 = 0{\cdot}9$.

Curing regime (relative humidity). Repair patches in the field can be cured in different ways. These are categorised into three main groups:[13] Group one involves keeping the surface of the repair patch moist by the use of ponding or continuous spraying; group two prevents moisture loss by covering the surface with polythene sheeting or leaving formwork in place; group three involves the use of curing compounds. Group one curing is most efficient but it is impractical in a repair situation. Group three is not as effective as group one but is more efficient than group two and has the advantage of needing no further supervision once the curing compound is applied. For this reason, and owing to their ease of application, curing compounds are the most commonly used technique for curing repair patches. Most of the curing compounds come in two grades: a standard grade

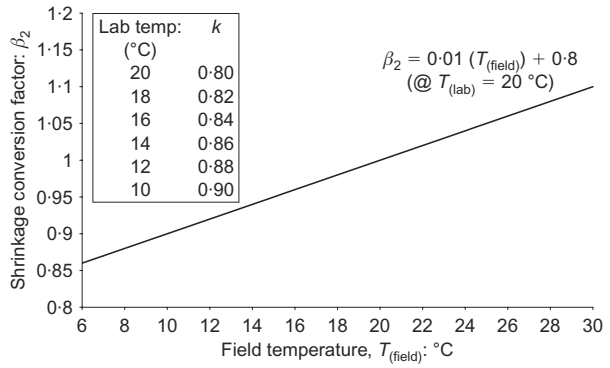

Fig. 4. Shrinkage conversion factor β_2 for temperature

having curing efficiency of 75% (relative humidity (RH) for curing = 75%) and a super grade having curing efficiency of 90% (tested in accordance with ASTM C309[14] or AS 3799).[15] The conservative value of 75%RH is assumed for the purposes of calculation in this paper.

The effect of applying a curing compound to a repair patch on its free shrinkage in the field can be calculated with reference to Fig. 5. The correction for RH differences between the laboratory and field conditions is based on a 2% decrease in shrinkage for each percent increase in RH to 70% and a 3% decrease in shrinkage for each percent increase in RH from 70% to 90%.[12] This results in an approximately linear relationship between the field relative humidity and the humidity correction factor β_3, as plotted in Fig. 5. The general equation representing the relationship is

$$\beta_3 = -\alpha(\%\text{RH}) + \eta \tag{24}$$

where %RH is the relative humidity in situ Fig. 5 gives the values of α and η and for laboratory relative humidity of 45, 55 and 65%. Values at other RH can be obtained by linear interpolation.

The repair patch made with material L4 was cured in the field using a curing compound and polythene sheeting. It is assumed that this gives a RH of 75% for field curing. The laboratory shrinkage data were obtained at 55%RH. Hence, from the appropriate graph in Fig. 5, the conversion factor, $\beta_3 \sim 0{\cdot}56$.

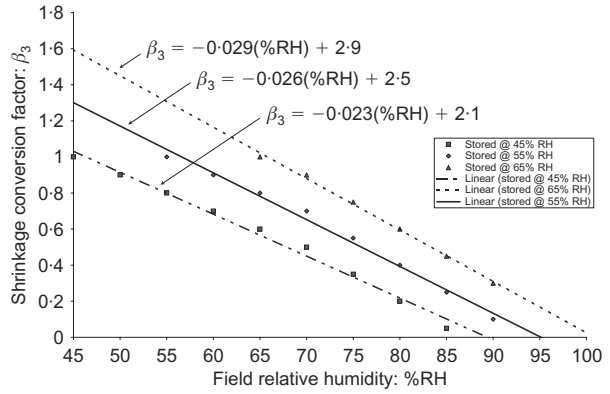

Fig. 5. Shrinkage conversion factor β_3 for relative humidity

Hence, the net field shrinkage of the repair patch made with repair material L4 can be calculated from the corresponding laboratory data of the material by applying the volume/surface, temperature and relative humidity correction factors β_1, β_2 and β_3 as follows:

Laboratory free shrinkage of material L4 at 100 days, $\varepsilon_{\text{shr(lab)}} = 782$ microstrain

Therefore

$$\begin{aligned}\varepsilon_{\text{shr(field)}} &= (\beta_1)(\beta_2)(\beta_3)(\varepsilon_{\text{shr(lab)}}) \\ &= (0{\cdot}6)(0{\cdot}9)(0{\cdot}56)(782) \\ &= 238 \text{ microstrain}\end{aligned}$$

Creep

Introduction. It was stated earlier that the incorporation of creep in the analysis would provide the most accurate estimation of stress at the substrate interface. The following section outlines this procedure, which introduces the creep coefficient of the repair material in the analysis through the effective elastic modulus (creep) approach.

Elastic modulus. The elastic modulus of the repair material was determined under compression in the laboratory in accordance with BS 1881.[8] The cylindrical test specimens measured 200 mm × 100 mm diameter and were tested at 28 days' age. However, since the repair material steadily develops its stiffness within the first month after application, and since creep relaxation is caused by restrained shrinkage tensile stresses, the 28-day compressive elastic modulus is converted to early-age tensile values by applying a conversion factor $\beta_{4(t)}$ (Fig. 6). $\beta_{4(t)}$ is determined on the following basis.

(*a*) The elastic modulus of a repair material at 7, 14 and 21 days equals 65, 85 and 96% of the 28-day value respectively.[16]
(*b*) The tensile elastic modulus of the repair material is approximately 9% lower than the compressive

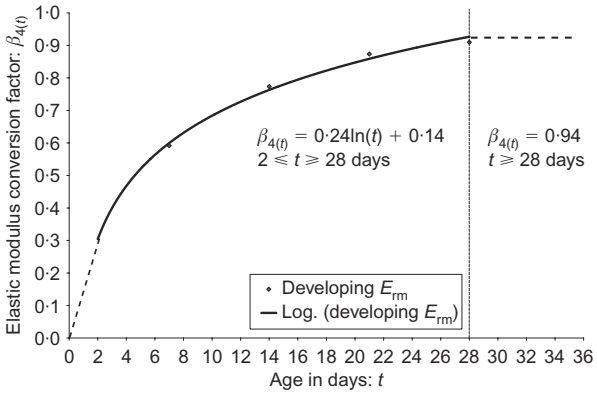

Fig. 6. Elastic modulus conversion factor $\beta_{4(t)}$ for age

value[17] which is generally provided by the manufacturers' data sheets.

(*c*) The tensile elastic modulus is used to calculate tensile stress by restrained shrinkage of the repair patch.

This information is represented graphically in Fig. 6 and the following best-fit equation is obtained

$$\beta_{4(t)} = 0{\cdot}24\ln(t) + 0{\cdot}14 \tag{25}$$

where t is the age of the repair patch in the range 2 to 28 days. The relationship in Fig. 6 yields a constant value for $\beta_{4(t)} \sim 0{\cdot}94$ at $t \geqslant 28$ days, reducing to approximately 0·3 at 2 days. The early-age tensile elastic modulus ($E_{\mathrm{rm}(t)}$) at time t days is, therefore, obtained from

$$E_{\mathrm{rm}(t)} = (E_{\mathrm{rm}})(\beta_{4(t)}) \tag{26}$$

where E_{rm} is the 28-day elastic modulus determined under compression in accordance with BS 1881[8] and $\beta_{4(t)}$ is obtained from Fig. 6 (or equation (25)).

Influence of creep on stiffness. The effect of creep is accounted for in the creep approach by determining the effective elastic modulus of the repair material, $E_{\mathrm{rm(eff)},t}$, from the following expression.[18]

$$E_{\mathrm{rm(eff)},t} = E_{\mathrm{rm}(t)}/(1 + \varphi) \tag{27}$$

where $E_{\mathrm{rm}(t)}$ is the elastic modulus of the repair material at time (equation (26)) and φ is the creep coefficient which is defined as

$$\varphi = \frac{\text{creep strain}}{\text{instantaneous elastic strain}} \tag{28}$$

The compressive creep strain of repair materials is obtained by standardised testing[19] and is assumed to equal tensile creep at the same stress/strength ratios.[20–22] Since the tensile stress/strength ratio of the repair material at the interface of the substrate concrete varies considerably within a steadily shrinking repair patch, an average stress/strength ratio of 30% was employed to determine φ. It will be shown below that the actual tensile stress/strength ratio in a repair patch (at the interface) varies considerably. Higher tensile stress/strength ratios (than 30%) would lead to relatively higher creep and higher relaxation of tensile stress, thereby providing a further factor of safety for crack control.

It is well established that cementitious materials exhibit more creep at early ages of loading. Fig. 7 shows the relationship between $\beta_{5(t)}$ and the age at which creep specimens are loaded, where

$$\beta_{5(t)} = \frac{\text{creep cofficient of specimens loaded at early age } (< 28 \text{ days})}{\text{creep coefficient of specimens loaded at 28 days age}} \tag{29}$$

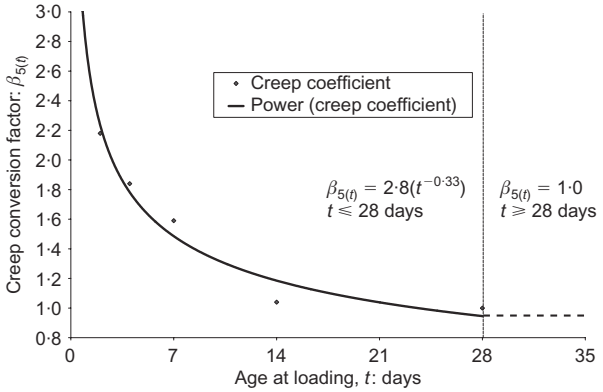

Fig. 7. Elastic modulus conversion factor $\beta_{5(t)}$ for early-age creep

The values of $\beta_{5(t)}$ for loading at 2, 4, 7, 14 and 28 days are plotted and the best-fit curve produced. Beyond 28 days age of loading, $\beta_{5(t)}$ remains unity.[23] At $t \leqslant 28$, $\beta_{5(t)}$ is given by the expression

$$\beta_{5(t)} = 2{\cdot}8(t^{-0{\cdot}33}) \tag{30}$$

where t is the age of the repair material in days when creep loading is applied. Thus, the creep coefficient at any age t, $\varphi_{(t)}$, is obtained from

$$\varphi_{(t)} = (\varphi)(\beta 5_{(t)}) \tag{31}$$

φ is obtained from equation (28) and $\beta_{5(t)}$ is obtained from Fig. 7 (or equation (30)). The effective elastic modulus, $E_{\mathrm{rm(eff)}}$, at $t \leqslant 28$ is, therefore, obtained by modifying equation (27) to take account of the elastic modulus–age relationship which gives factor ($\beta_{4(t)}$) and the effect of early age loading on creep which gives factor $\beta_{5(t)}$. The resulting expression for $E_{\mathrm{rm(eff)}}$, at time t is given by

$$E_{\mathrm{rm(eff)},t} = (E_{\mathrm{rm}})(\beta_{4(t)})/[1 + (\varphi)(\beta_{5(t)})] \tag{32}$$

With regard to the example of the field repair patch made with repair material L4, the restrained shrinkage strain transfer occurs over approximately a three-month period,[5] hence $t \geqslant 28$ days. Referring to the graph in Fig. 6, $\beta_{4(t)} \sim 0{\cdot}94$ and $\beta_{5(t)} \sim 1{\cdot}0$ from the graph in Fig. 7. The creep coefficient, φ (equation (28)), for this material is 0·89 from laboratory tests (φ was not available from the repair material manufacturer's literature). Therefore, from equation (32), the effective elastic modulus at $t > 28$ days is

$$E_{\mathrm{rm(eff)},t\geqslant 28} = (29{\cdot}1)(0{\cdot}94)/[1 + (0{\cdot}89)(1{\cdot}0)]$$

$$= 14{\cdot}5 \text{ kN/mm}^2$$

Validation

Interfacial stresses

A summary of the interfacial stresses calculated in repair patches of bridge elements, made with four re-

pair materials (L4, L3, L2 and G1) are given in Table 1. The material identification is given in column 1. Stresses are calculated at both the substrate concrete and repair material interface ('subs' and 'rm @ interface' respectively, Table 1, column 2). Stresses modified by the creep coefficient (creep approach) are given in column 3 and are calculated at arbitrary ages of 14, 90 and 182 days after application (0·5, 3 and 6 months respectively). This is the most rigorous method of stress analysis presented and leads to the highest accuracy. The interfacial stresses at these ages are used to illustrate the variation in tensile stress/strength ratios that occur after application of patch repairs (further details are given below). Interfacial stresses calculated by the elastic approach (i.e. using E_{rm} and not $E_{rm(eff)}$) at age 182 days only are presented in column 4 and are consistently higher than those predicted by the creep approach at 182 days (column 3 and Fig. 8). Referring to columns 3, 4 in Table 1 and Fig. 8, the rm @ interface (creep approach) stresses at age 182 days are approximately half those of the elastic approach. It is recommended, therefore, to use the elastic approach in design of patch repairs for two reasons. First, creep properties of repair materials are generally unavailable in manufacturers' literature and second, the elastic approach has an in-built factor of safety of approximately two.

The substrate concrete stresses are marginally higher using the elastic approach (compare subs stresses at 182 days in columns 3 and 4 in Table 1 and Fig. 8). The prediction of compressive stress in the substrate concrete is less important for the design of a patch repair since the magnitude of compressive stress in a repair patch is insignificant relative to the compressive strength of a typical repair material which exceeds 30 N/mm^2 at 28 days. The semi-empirical method (Fig. 8) provides a reasonable estimation of interfacial stresses but the more rigorous creep approach is preferred to ensure higher accuracy.

Tensile stress/strength ratios

Information on the direct tensile strength of repair materials is largely unavailable in the data sheets, although indirect tensile properties in the form of modulus of rupture and cylinder splitting strength are sometimes available. The tensile strength of the four repair materials under consideration is estimated from a relationship between the direct tensile strengths and cube crushing strength for concrete mixes.[24] All repair materials are cementitious based and further details can be obtained elsewhere. [5]

The ratio of average compressive strength for a number of repair materials at any age t, $f_{cu(t),}$, in relation to the average 28-day compressive strength, $f_{cu(28)}$, is given in Fig. 9. This relationship is based on the average compressive strength (up to age 28 days) of the four repair materials considered in this paper and is extrapolated thereafter based on a Portland cement concrete[17] for the purpose of this paper. It is used to provide an estimation of the compressive strengths of the repair materials at 14, 90 and 182 days after application. Referring to Fig. 9, at age 14 days, the ratio $f_{cu(14)}/f_{cu(28)}$ is approximately 0·88. $f_{cu(90)}/f_{cu(28)}$ is approximately 1·16 at age 90 days and at 182 days the ratio $f_{cu(182)}/f_{cu(28)}$ is approximately 1·2. The 28-day cube strengths listed in column 6, Table 1, obtained from the manufacturers' literature, are therefore multiplied by 0·88, 1·16 and 1·2 to give an estimation of the compressive strength at 14, 90 and 182 days respectively (Table 1).

An estimation of the tensile strength at the selected ages is given in column 7. It is based on a relationship between compressive and direct tensile strengths for concrete which is given by

$$\sigma_{t(t)} = 0{\cdot}27 f_{cu(t)}^{0{\cdot}59} \tag{33}$$

where $\sigma_{t(t)}$ is the estimated tensile stress at time t_{24} ($t = 14$, 90 and 182 days).

The estimated tensile strengths at 14, 90 and 182 days age are listed in column 7 of Table 1. The tensile stress of the repair material at the three ages is listed in column 3. The resulting tensile stress/strength ratios at the repair material interface are given in column 8. It is clear from column 8 that the tensile stress/strength ratios are lower at early ages (average 19% at 14 days) but increase with time to average 49% at 14 days and 48% at 182 days. These figures indicate that at early ages the elastic modulus and shrinkage properties of the repair materials are developing rapidly while creep relaxation is also maximum (see $\beta_{5(t)}$, Fig. 7), hence high creep is offsetting the restrained shrinkage stresses. At later stages (90 and 182 days), the elastic modulus and shrinkage properties of the repair materials have stabilised and relaxation of stress due to high creep rates no longer applies. Higher stresses and consequently, higher tensile stress/strength ratios result but the magnitudes are insufficient to cause tensile cracking due to restrained shrinkage.

To ensure that the repair patch remains crack-free, the tensile stress/strength ratio (after creep relaxation) must remain below 100% (or 50% to apply a factor of safety of 2). This can be achieved through designing the repair patch in accordance with the recommendations given in this paper.

Conclusions

The following conclusions are based on the information presented in the paper.

(*a*) Laboratory shrinkage of repair materials, $\varepsilon_{shr(lab)}$, can be related to in situ shrinkage in the field, $\varepsilon_{shr(field)}$, by applying three conversion factors from approved methods, namely β_1 for volume/surface

Table 1. Validation of procedures

Column 1	Column 2	Column 3			Column 4	Column 5	Column 6				Column 7			Column 8		
Material	Location	Creep approach* (equations (15) and (16)): N/mm^2			Elastic approach† (equations (15) and (16)): N/mm^2	Semi-empirical approach† (equations (19) and (21)): N/mm^2	Estimated cube strength, $f_{cu(t)}$‡ (Fig. 9): N/mm^2				Estimated tensile strength, $\sigma_{t(t)}$ (equation (33)): N/mm^2			$\frac{\text{tensile stress, column 3}}{\text{tensile strength, columnn 7}}$: %		
		14 days	90 days	182 days	182 days	182 days	28 days§	14 days	90 days	182 days	14 days	90 days	182 days	14 days	90 days	182 days
L4	subs	+1·4	+2·4	+2·5	+3·0	+3·9	60	53	70	72	−2·8	−3·3	−3·4	27	48	47
	rm@interface	−0·7	−1·6	1·6	−3·3	−2·1										
L3	subs	+0·4	+2·0	+2·0	+2·6	+2·4	35	31	41	42	−2·0	−2·4	−2·4	9	46	46
	rm@interface	−0·2	−1·1	−1·1	−2·8	−3·0										
L2	subs	+1·0	+1·4	+1·4	+1·7	+2·8	60	53	70	72	−2·8	−3·3	−3·4	13	24	24
	rm@interface	−0·5	−0·8	−0·8	−1·9	−0·6										
G1	subs	+2·1	+4·0	+4·0	+4·7	+3·1	60	53	70	72	−2·8	−3·3	−3·4	27	79	76
	rm@interface	−1·1	−2·6	−2·6	−5·0	−6·8										
														19	49	48
														Averages		

* $(E_{rm(eff),t})(\varepsilon_{rm(tens)})$
† $(E_{rm})(\varepsilon_{rm(tens)})$
‡ Strength extrapolated from manufacturers' 28-day strengths[18]
§ Manufacturers' 28-day strengths

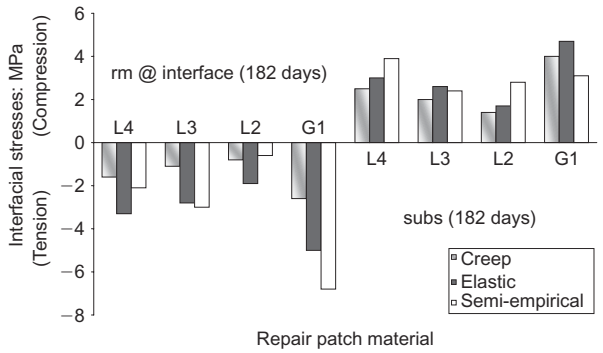

Fig. 8. Comparison of stresses at 182 days after application

correction, β_2 for temperature correction and β_3 for relative humidity correction.

(*b*) The interfacial compressive stress in the substrate concrete due to the transfer of shrinkage from the repair material can be analytically determined from

$$\sigma_{\text{sub(shr)}} = \frac{F_{\text{shr}}}{b\sqrt{m}d_{\text{rm}}} + \frac{E_{\text{sub}}\sqrt{m}d_{\text{rm}}}{2R}$$

(*c*) The interfacial elastic tensile stress in the repair material, when relaxation due to creep is neglected, can be analytically determined from

$$\sigma_{\text{rm(shr)}} = -\frac{F_{\text{shr}}}{bd_{\text{rm}}} - \frac{E_{\text{rm}}d_{\text{rm}}}{2R}$$

(*d*) The interfacial relaxed tensile stress in the repair material, when the effects of creep are considered, can be analytically determined by replacing E_{rm} with $E_{\text{rm(eff)},t}$ as follows

$$\sigma_{\text{rm(shr)}} = -\frac{F_{\text{shr}}}{bd_{\text{rm}}} - \frac{E_{\text{rm(eff)},t}(d_{\text{rm}})}{2R}$$

where

$$E_{\text{rm(eff)},t} = (E_{\text{rm}})(\beta 4_{(t)})/[1 + (\varphi)(\beta_{5(t)})]$$

(*e*) The interfacial compressive stress in the substrate concrete due to the transfer of shrinkage from the repair material can be semi-empirically determined from $\sigma_{\text{sub(shr)}} = (\varepsilon_{\text{sub(shr)}})(E_{\text{sub}})$.

(*f*) The interfacial tensile stress in the repair material can be semi-empirically determined from $\sigma_{\text{rm(shr)}} = (\varepsilon_{\text{rm(tens)}})(E_{\text{rm}})$.

(*g*) The tensile stress/tensile strength ratios for repair materials specified in accordance with the recommendations given in this paper are low in the early ages after application owing to high creep and lower elastic modulus and shrinkage. These ratios increase over time but should remain below 100% in order to prevent restrained shrinkage cracking (or 50% if a factor of safety of 2 is to be assumed).

Acknowledgements

This paper is based on a LINK TIO funded project entitled ‘Long-term performance of concrete repair in highway structures’. The partners in the project were

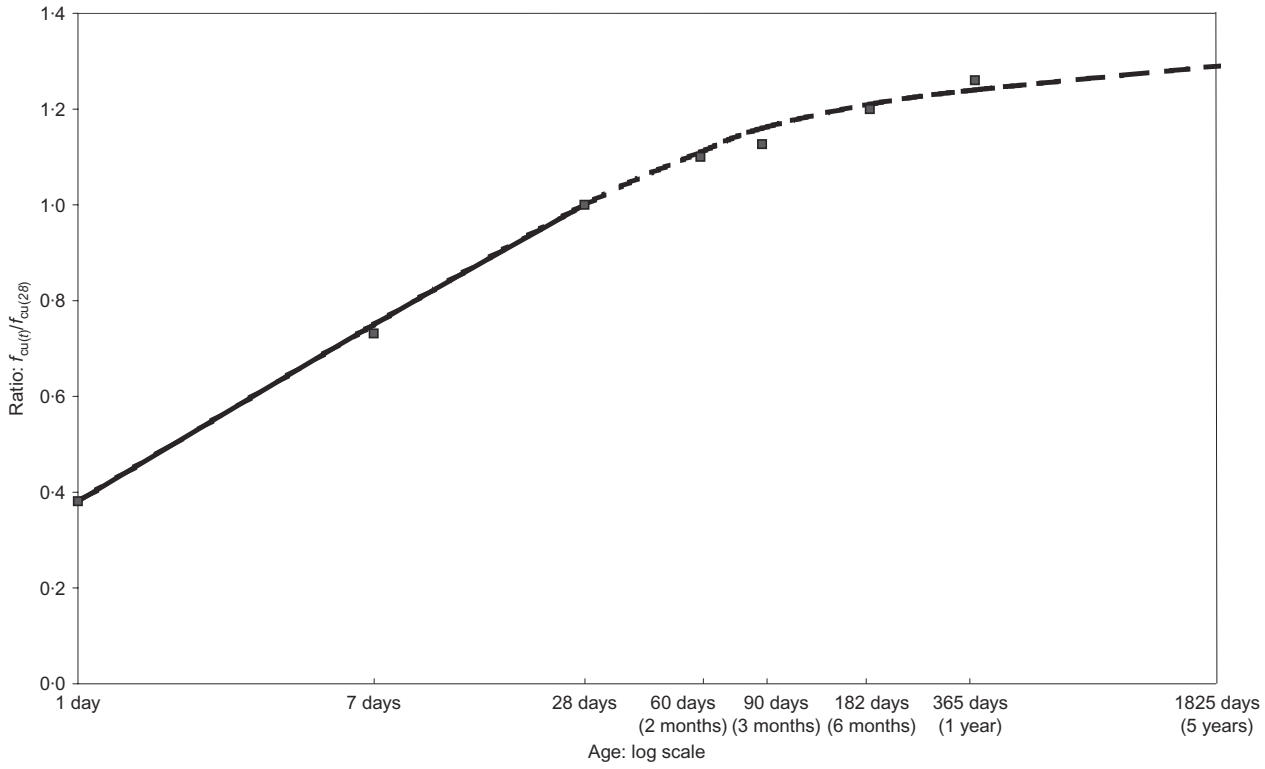

Fig. 9. Average compressive strength development for a repair material

Sheffield Hallam University, V.A. Crookes (Contracts) Ltd, Flexcrete Ltd, M. J. Gleeson Group plc. The contribution of all project partners, the former Department of Transport, the Highways Agency and local authorities (Nottinghamshire County Council, Sheffield City Council) are gratefully acknowledged.

References

1. Emmons P. H., Vaysburd A. M. and McDonald J. E. Concrete repair in the future turn of the century—any problems? *Concrete International,* 1994, **16**, No. 3, 42–49.
2. Mangat P. S. and O'Flaherty F. J. Factors affecting the efficiency of repair to propped and unpropped bridge beams. *Magazine of Concrete Research*, 2000, **52**, No. 4, 303–319.
3. Mangat P. S. and O'Flaherty F. J. Serviceability characteristics of flowing repairs to propped and unpropped bridge structures. *Materials and Structures*, 1999, **32**, No. 223, 663–672.
4. Mangat P. S. and O'Flaherty, F. J. Influence of elastic modulus on stress redistribution and cracking in repair patches. *Cement and Concrete Research*, 2000, **30**, No. 1, 125–136.
5. Mangat P. S. and O'Flaherty F. J. Long-term performance of high stiffness repairs in highway structures. *Magazine of Concrete Research*, 1999, **51**, No. 5, 325–339.
6. O'Flaherty F. J. and Mangat P. S. Recommendations for the European Prestandard for concrete repair. *RILEM 2nd International Workshop on Life Prediction and Aging Management of Concrete Structures*, Paris, France, 5–6 May 2003, pp. 237–245.
7. Mangat P. S. and O'Flaherty F. J. Analysis of interfacial shrinkage stress in patch repairs. *Magazine of Concrete Research*, 2003, **56**, No. 7, 375–386.
8. British Standards Institution. BS 1881. *Method for determination of static modulus of elasticity in compression, Part 121*. BSI, London, 1983.
9. Mangat P. S. and Limbachiya M. K. Repair materials properties which influence long-term performance of concrete structures. *Construction and Building Materials,* 1995, **9**, No. 2, 81–90.
10. Mangat P. S. and Limbachiya M. K. Repair material properties for effective structural application. *Cement and Concrete Research,* 1997, **27**, No. 4, 601–617.
11. Dector M. H. and Lambe R. W. New materials for concrete repair–development and testing. *The Indian Concrete Journal,* 1993, **67**, No. 10, 475–480.
12. Kong F. K. and Evans R. H. *Reinforced and Prestressed Concrete*, 3rd edn. Van Nostrand Reinhold, New York, 1987.
13. Curing, Cement and Concrete Association of New Zealand. *Site Concreting, SC 4* (www.holcim.com/Upload/NZ/Publications/ECS_Curing%20of%20Concrete.pdf).
14. American Society for Testing Materials. *Standard specification for liquid membrane-forming compounds for curing concrete*. ASTM C 309–97. ASTM, Philadelphia, PA, USA, 1997.
15. Australian Standard. *Liquid membrane-forming compounds for concrete*. Standards Australia, Sydney, 1998, AS 3799–1998.
16. Pinelle D. J. Curing stresses in polymer modified repair mortars. *Cement, Concrete and Aggregates, CCAGDP*, 1995, **17**, No. 2, 195–200.
17. Brooks J. J. and Neville A. M. A comparison of creep, elasticity and strength of concrete in tension and in compression. *Magazine of Concrete Research*, 1978, Vol. **29**, No. 100, 131–141.
18. Mosley W. H. and Bungey J. H. *Reinforced Concrete Design*, 4th edn. McMillan, London, 1990, p. 362.
19. Illston J. M. and Pomeroy C. D. Recommendations for a standard creep test. *Concrete*, 1975, **9**, No. 12, 24–25.
20. Illston J. M. The creep of concrete under uniaxial tension. *Magazine of Concrete Research*, 1965, **17**, No. 51, 77–84.
21. Glanville W. H. and Thomas F. G. *Further Investigations on the Creep or Flow of Concrete under Load.* Building Research Technical Paper No. 21. HMSO, London, 1939, pp. 5–8.
22. Hanson J. A. *A 10-year study of creep properties of concrete.* United States Department of the Interior, Bureau of Reclamation, July 1953, Laboratory Report, No. SP-38.
23. Yuan Y. S. and Marosszeky M. Major factors affecting the performance of structural repair. *Proceedings of the ACI International Conference on Evaluation and Rehabilitation of Concrete Structures and Innovations in Design*. ACI-SP128, Vol. 2. American Concrete Institute, Detroit, 1991, pp. 819–837.
24. Brooks J. J. and Neville A. M. A comparison of creep, elasticity and strength of concrete in tension and in compression. *Magazine of Concrete Research*, 1977, **29**, No. 100, 131–141.

Discussion contributions on this paper should reach the editor by 1 August 2006